Switching off calcium-dependent inactivation in L-type calcium channels by an autoinhibitory domain

Christian Wahl-Schott, Ludwig Baumann, Hartmut Cuny, Christian Eckert, Kristina Griessmeier, and Martin Biel*

Department Pharmazie – Zentrum für Pharmaforschung, Ludwig-Maximilians-Universität München, Butenandtstrasse 7, 81377 Munich, Germany

Edited by Harald Reuter, University of Bern, Bern, Switzerland, and approved August 25, 2006 (received for review June 3, 2006)

The retinal L-type Ca^{2+} channel Cav1.4 is distinguished from all other members of the high voltage-activated (HVA) Ca^{2+} channel family by lacking Ca^{2+}-calmodulin-dependent inactivation. In synaptic terminals of photoreceptors and bipolar cells, this feature is essential to translate graded membrane depolarizations into sustained Ca^{2+} influx and tonic glutamate release. The sequences conferring Ca^{2+}-dependent inactivation (CDI) are conserved throughout the HVA calcium channel family, raising the question of how Cav1.4 manages to switch off CDI. Here, we identify an autoinhibitory domain in the distal C terminus of Cav1.4 that serves to abolish CDI. We show that this domain (ICDI, inhibitor of CDI) uncouples the molecular machinery conferring CDI from the inactivation gate by binding to the EF hand motif in the proximal C terminus. Deletion of ICDI completely restores Ca^{2+}-calmodulin-mediated CDI in Cav1.4. CDI can be switched off again in the truncated Cav1.4 channel by coexpression of ICDI, indicating that ICDI works as an autonomous unit. Furthermore, we show that in the Cav1.2 L-type Ca^{2+}-channel replacement of the distal C terminus by the corresponding sequence of Cav1.4 is sufficient to block CDI. This finding suggests that autoinhibition of CDI can be introduced principally into other Ca^{2+} channel types. Our data provide a previously undescribed perspective on the regulation of HVA calcium channels by Ca^{2+}.

calmodulin | Cav1.4 | retina | Ca channels

Synaptic release of neurotransmitters critically depends on the influx of Ca^{2+} through voltage-gated Ca^{2+} channels. In most neurons of the CNS, synaptic Ca^{2+} influx has to decay rapidly to faithfully translate trains of action potentials into corresponding quantal release of synaptic vesicles (1). Fast channel inactivation is principally conferred by voltage but is enhanced by an intrinsic feedback mechanism designated as Ca^{2+}-dependent inactivation (CDI) by which Ca^{2+} limits its own influx (2). In contrast to most neurons, retinal photoreceptors and bipolar cells generate graded electrical responses (3, 4) and, hence, require a sustained rather than a transient Ca^{2+} influx for neurotransmitter release (5, 6). Indeed, calcium currents characterized in retinal cells reveal slow inactivation kinetics and are virtually devoid of CDI (7–9). Two members of the L-type subclass of high voltage-activated calcium channels have been described in ribbon synapses of photoreceptors and bipolar cells, Cav1.4 (10–12) and Cav1.3 (12, 13). Genetic studies indicate that the major channel mediating synaptic Ca^{2+} influx in rod photoreceptors and rod bipolar cells is Cav1.4 (10, 11). The electrophysiological properties of heterologously expressed Cav1.4 are consistent with those of native retinal calcium currents (14–16). In particular, Cav1.4 inactivates slowly and lacks CDI. At first glance, this finding is surprising given that Cav1.4 shares high sequence homology with other high voltage-activated calcium channels that display profound CDI. In this study, we set out to analyze the mechanism and the structural basis underlying this important functional difference.

Results

Fig. 1*A* shows current traces of the CDI-displaying calcium channel, Cav1.2, expressed in HEK293 cells. In the presence of Ba^{2+} inactivation is relatively slow and depends only on the membrane potential (voltage-dependent inactivation). If Ca^{2+} is the permeating ion, the channel inactivates much faster because of the presence of CDI. Pure CDI can be quantified by the *f* value, which corresponds to the difference in normalized I_{Ba} and I_{Ca} remaining after 300 ms of depolarization. In Cav1.2, like in other channels with CDI, *f* values reveal a U-shaped dependence on the test pulse voltage (17), reaching a maximal value (f_{max}) of ≈0.3 (Fig. 1*B*). The Ca^{2+}-sensing apparatus of Cav1.2 resides in the proximal C terminus of the channel (17–25) (Fig. 6, which is published as supporting information on the PNAS web site). It comprises a sequence (pre-IQ and IQ segment) that binds calmodulin (CaM), which is the primary Ca^{2+} sensor of the channel. In addition, it contains an EF hand motif that allosterically couples the Ca^{2+}-sensing apparatus with the inactivation gate of the channel. These domains are highly conserved in the retinal Cav1.4 channel. Surprisingly, however, this channel does not display CDI. I_{Ba} and I_{Ca} of Cav1.4 show the same kinetics (Fig. 1*C*), and the *f* value is zero over the whole voltage range tested (Fig. 1*D*).

We first considered that Cav1.4 may lack CDI because it is deficient in binding CaM. To test for this option, we performed pulldown assays with GST fusion proteins containing C-terminal fragments of Cav1.2 and Cav1.4 and purified CaM (Figs. 1*E*; see Fig. 7*A*, which is published as supporting information on the PNAS web site). CaM bound to the proximal C terminus of both channels (CT1.2-1667Stop and CT1610Stop) in a Ca^{2+}-dependent fashion. Binding of CaM also was observed to the full-length C terminus of Cav1.4 (data not shown). By contrast, no interaction was seen with the distal C termini, comprising sequences downstream of the IQ segment (CT1.2-1667–2166 and CT1610–1984). The absence of signals in the presence of EGTA did not necessarily mean that Ca^{2+}-free CaM (apocalmodulin) is principally insufficient to bind to Cav1.4 and Cav1.2 because some basal Ca^{2+} may be transiently required for the proper folding of a binding pocket for apocalmodulin (23, 24). To explore this issue, we performed coimmunoprecipitations (Co-IPs) in HEK293 cells by using a CaM mutant (CaM_{1234}) that is deficient for Ca^{2+} binding serving as an apocalmodulin surrogate (26). In these assays, CaM_{1234} bound to the C termini of either Cav1.2 or Cav1.4 channels strongly supports the hypothesis that apocalmodulin indeed can bind to both channels at basal Ca^{2+} conditions (Fig. 1*F*). Together, these findings excluded loss of the calcium sensor CaM as a mechanism explaining Ca^{2+} insensitivity of Cav1.4 but rather suggested that CDI may be actively masked by an inhibitory channel domain. Indeed,

Author contributions: C.W.-S. and L.B contributed equally to this work; C.W.-S., L.B., H.C., and M.B. designed research; C.W.-S., L.B., H.C., C.E., and K.G. performed research; C.W.-S., L.B., H.C., K.G., and M.B. analyzed data; and C.W.-S. and M.B. wrote the paper.

The authors declare no conflict of interest.

This article is a PNAS direct submission.

Abbreviations: CaM, calmodulin; CDI, calcium-dependent inactivation; Co-IP, coimmunicipation; ICDI, inhibitor of CDI.

*To whom correspondence should be addressed. E-mail: mbiel@cup.uni-muenchen.de.

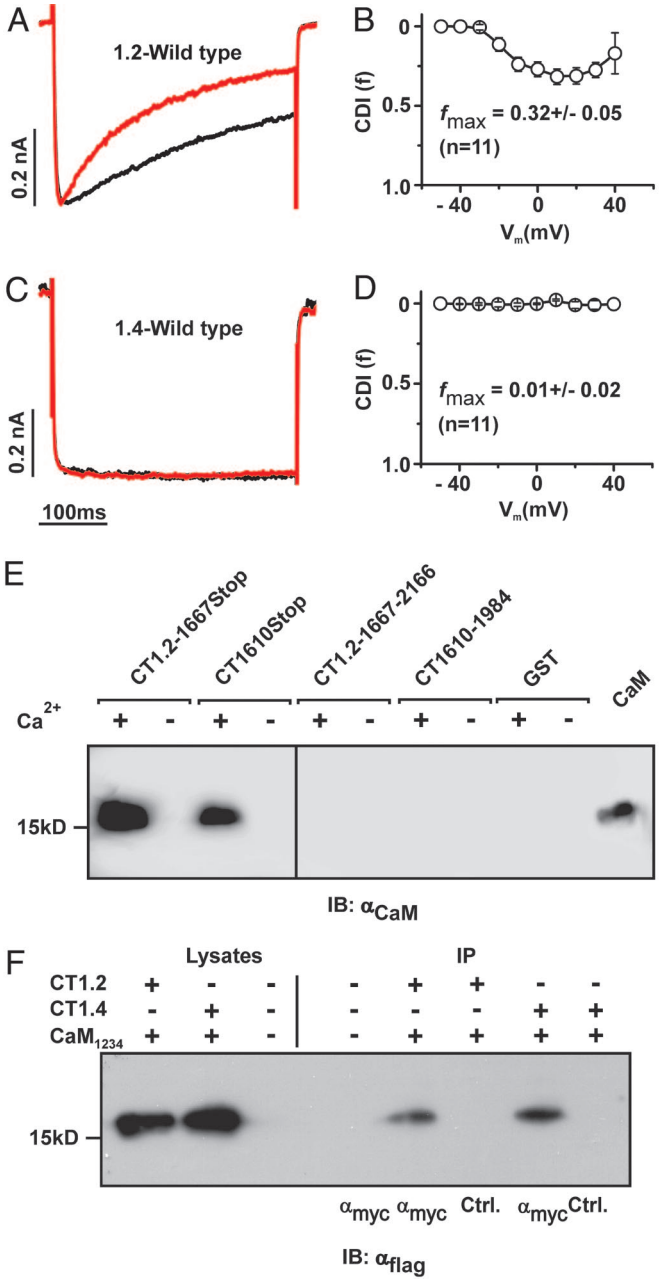

Fig. 1. Cav1.4 binds CaM but does not reveal CDI. (*A*) Representative traces of I_{Ca} (red traces) and I_{Ba} (black traces) through Cav1.2 evoked by stepping from a holding potential of −80 mV to +10 mV. Current traces were normalized to peak current. Throughout, Ba^{2+} traces for CDI are scaled to match Ca^{2+} traces (scale bar) (*B*) Strength of CDI, *f*, in relation to voltage for Cav1.2. f_{max} is the maximal *f* value, *n* number of cells. (*C* and *D*) Representative I_{Ca} and I_{Ba} currents (*C*) and voltage-dependence of *f* for Cav1.4 (*D*). (*E*) GST fusion proteins containing fragments corresponding to the proximal and distal C terminus of Cav1.2 (CT1.2-1667Stop and CT1.2-1667–2166) or Cav1.4 (CT1610Stop and CT1610–1984) were incubated with CaM in the presence (+) or absence (−) of Ca^{2+}. Immunoblotting was performed with an anti-CaM antibody. In the last lane, 1 μg of CaM was blotted to demonstrate specificity of the assay. (*F*) Co-IP of HEK293 cells coexpressing triple flag-tagged CaM_{1234} together with the myc-tagged full-length C terminus of Cav1.2 (CT1.2) or Cav1.4 (CT1.4). Lysates were immunoprecipitated with anti-myc (lanes 5 and 7) or anti-GST (control, lanes 6 and 8), blotted and probed with anti-flag. Lane 3 and 4: negative control.

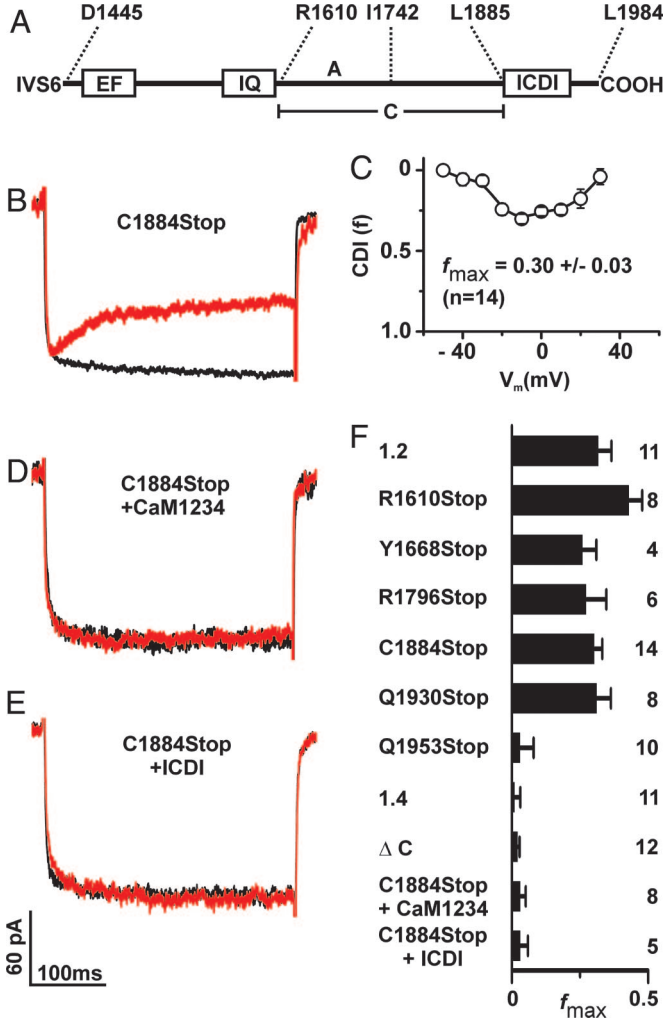

Fig. 2. The ICDI domain is required to block CDI in Cav1.4. (*A*) Scheme of the Cav1.4 C terminus starting after the IVS6 segment. Numbers delineate the borders of peptides A, C, and ICDI. (*B*) Representative traces of I_{Ca} (red trace) and I_{Ba} (black trace) through a truncated Cav1.4 channel lacking ICDI (C1884Stop). (*C*) Voltage-dependence of *f* for C1884Stop. (*D* and *E*) Coexpression of C1884Stop and a dominant negative CaM_{1234} (*D*) or ICDI (*E*). (*F*) f_{max} for wild-type and mutant channels and for coexpression experiments as indicated.

when the last 100 aa were removed from the C terminus of Cav1.4 (C1884Stop), CDI was recovered fully (Fig. 2*A* and *B*). Like the Cav1.2 channel C1884Stop showed fast inactivation in the presence of Ca^{2+} that was best fitted with two time constants, whereas there was no inactivation with Ba^{2+} (Table 1 and Fig. 8*A*, which are published as supporting information on the PNAS web site). CDI also was present in other Cav1.4 channels with truncations between the IQ segment and C1884 (R1610Stop, Y1668Stop, and R1796Stop) (Fig. 2 *A* and *F*). The *f* value of C1884Stop showed the typical U-shaped voltage dependence, and f_{max} was virtually identical to that of Cav1.2 [0.3 ± 0.03 (n = 14); Figs. 2 *C* and *F* and 8*A* and Table 1]. To demonstrate that CDI in C1884Stop was mediated by CaM, we coexpressed the channel together with the negative-dominant CaM mutant CaM_{1234}. Under these conditions, no CDI was observed (Figs. 2 *D* and *F* and 8*A* and Table 1). Finally, we coexpressed C1884Stop with a peptide corresponding to the last 100 aa of Cav1.4 (ICDI, inhibitor of CDI) in HEK293 cells. Again, CDI was totally absent (Figs. 2 *E* and *F* and 8*A*), indicating that ICDI was acting as an independent protein unit and was sufficient to block CDI in Cav1.4. In support of this model, a Cav1.4 mutant in which ICDI was directly attached to the IQ motif also showed no CDI (ΔC, Figs. 2*F* and 8*A*). We

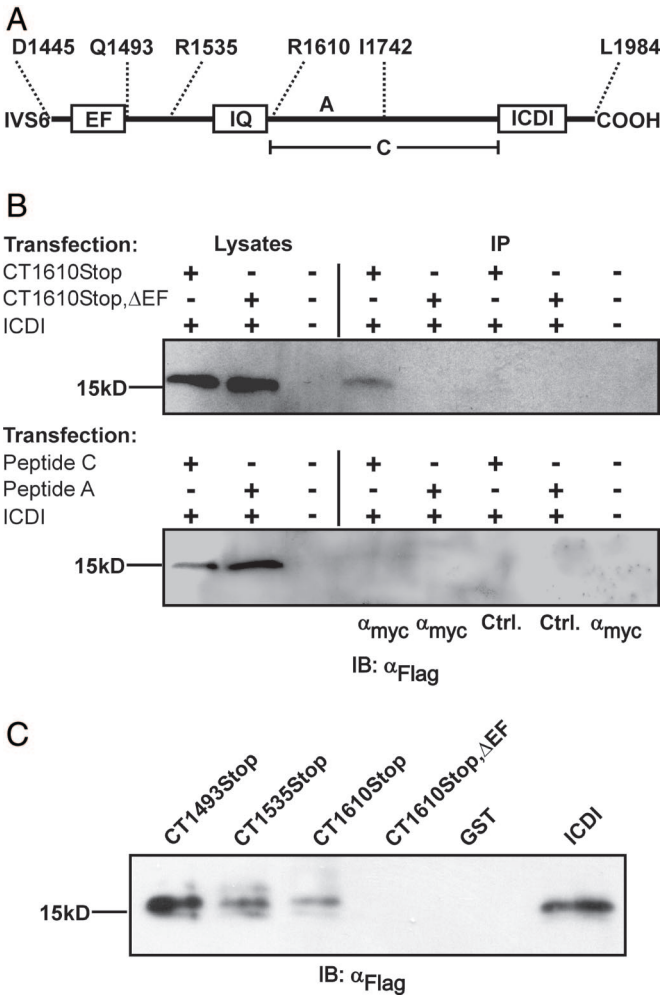

Fig. 3. The ICDI domain binds to the EF hand motif of Cav1.4. (*A*) Scheme of the Cav1.4 C terminus starting after the IVS6 segment. (*B Upper*) Co-IP of HEK293 cells coexpressing triple flag-tagged ICDI together with the myc-tagged CT1610Stop or CT1610Stop,ΔEF. Lysates were immunoprecipitated with anti-myc (lanes 4 and 5) or anti-ras (control, lanes 6 and 7), blotted and probed with anti-flag. Lane 8: negative control. (*B Lower*) Immunoprecipitation of HEK293 cells expressing ICDI and myc-tagged peptides C or A. Co-IP has been carried out as in *Upper*. (*C*) ICDI interaction assay with GST-tagged fragments of the proximal C terminus. GST fusion proteins were incubated with bacterial lysates containing flag-tagged ICDI. Immunoblotting was performed with an anti-flag antibody. In the last lane, pure ICDI was blotted to demonstrate specificity of the assay. Each experiment was repeated at least three times.

constructed two additional Cav1.4 truncations to further narrow down the minimal sequence required for block of CDI (Figs. 2*F* and 8*A*). Q1930Stop showed CDI, whereas Q1953Stop did not, indicating that the sequence stretch between amino acids 1930–1953 is of particular importance in blocking CDI.

We next asked whether the ICDI domain could interact with the Ca^{2+}-sensing apparatus of Cav1.4. To explore this issue, we performed Co-IPs with myc-tagged C-terminal fragments of Cav1.4 and triple-flag-tagged ICDI (Figs. 3 *A* and *B*; see Fig. 9, which is published as supporting information on the PNAS web site). As proposed, ICDI specifically bound to the proximal C terminus of Cav1.4 (Fig. 3*B Upper*, lane 4). However, ICDI no longer interacted with this domain when the EF hand motif was deleted (Fig. 3*B Upper*, lane 5). Moreover, no interaction was observed between ICDI and peptides A and C that were derived from the distal C terminus of Cav1.4 (Fig. 3 *A* and *B Lower*). This important finding was confirmed by a series of pulldown assays with bacterial GST fusion proteins (Fig. 7). Finally, to prove directly that ICDI binds to the EF hand, GST pulldowns were performed with peptides containing the EF hand or the EF hand and the N-terminal half of the PreIQ (Fig. 3C, CT1493Stop and CT1535Stop). Both peptides bound the ICDI, indicating that the EF hand serves as target sequence of ICDI. Analysis of the primary sequence indicates that ICDI has an α helical structure [predicted by PhD analysis (27), confidence level >82%]. Given that the EF hand also contains helices (25), it is tempting to speculate that ICDI and EF hand can form a paired helix complex. Considering the central role of the EF hand as a general downstream transduction element for CDI (19, 24, 28–30), we propose that the interaction between ICDI and EF hand uncouples the Ca^{2+}-sensing apparatus from the inactivation gate of Cav1.4.

We were wondering whether the inactivation of Cav1.2 could be rendered insensitive to Ca^{2+} by replacing C-terminal portions of this channel by corresponding sequences of Cav1.4. To this end, we constructed a series of Cav1.2-1.4 chimeras and deletion mutants (Fig. 4*A*) and determined the inactivation parameters of these channels (Fig. 4*F* and 8*B* and Table 1). When the complete C terminus of Cav1.2 was replaced by the corresponding sequence of Cav1.4 (1.2-CT1.4) CDI was completely abolished (Fig. 4*F*). Importantly, a Cav1.2-1.4 chimeric channel in which only the portion downstream of the IQ motif was derived from Cav1.4 (1.2-C+ICDI1.4) also lacked CDI, confirming our concept that the distal C terminus of Cav1.4 is sufficient to block CDI (Fig. 4 *B*, *C*, and *F* and Table 1). However, Cav1.2 channels in which only the last 149 aa were replaced by ICDI of Cav1.4 (1.2-ICDI1.4) or where ICDI was fused directly to the IQ motif (1.2ΔC-ICDI1.4) still displayed CDI (Fig. 4 *D* and *F* and Table 1). To abolish CDI, it was necessary to introduce the peptide A of Cav1.4 together with ICDI into the Cav1.2 backbone. The resulting chimera (1.2-A+ICDI1.4) passed a fast inactivating current with kinetics that were in the range of those observed for I_{Ca} of wild-type Cav1.2 (Fig. 4 *E* and *F* and Table 1). Attempts to further narrow down the borders of peptide A failed, suggesting that the whole sequence is needed for blocking CDI (data not shown). Notably, however, in the absence of ICDI, peptide A was not sufficient to block CDI (chimera 1.2-A1.4; Fig. 4F). In conclusion, ICDI is obligatorily required to block CDI in Cav1.2. However, unlike in Cav1.4, in the Cav1.2 backbone, it needs the cooperation of peptide A. Because peptide A does not bind ICDI (Figs. 3*B* and 7*B*), we propose that it supports the inhibitory action of ICDI via an indirect mechanism.

Discussion

Here, we demonstrate that the retinal Cav1.4 channel utilizes the intramolecular interaction between an autoinhibitory domain present in the distal C terminus (ICDI) and the EF hand in the proximal C terminus to functionally block CaM-mediated CDI. Our data have profound mechanistic consequences with regard to the regulation of L-type calcium channels by Ca^{2+}. According to established models, CDI of high voltage-activated Ca^{2+} channels requires functional interaction between the channel core and the proximal C terminus that is transduced by the EF hand (refs. 24, 28, and 29; Fig. 5*A*). At rest, when cytosolic Ca^{2+} levels are low, the EF hand is presumed to interact weakly with the cytoplasmic gate in a manner that permits ready opening of the gate (29), stabilizes the open state, or helps to create a deceleratory signal to retard channel inactivation (24, 30). Voltage induces a slow conformational change that induces closure of the pore (voltage-dependent inactivation). Interaction of Ca^{2+} with prebound CaM induces a conformational change in the EF

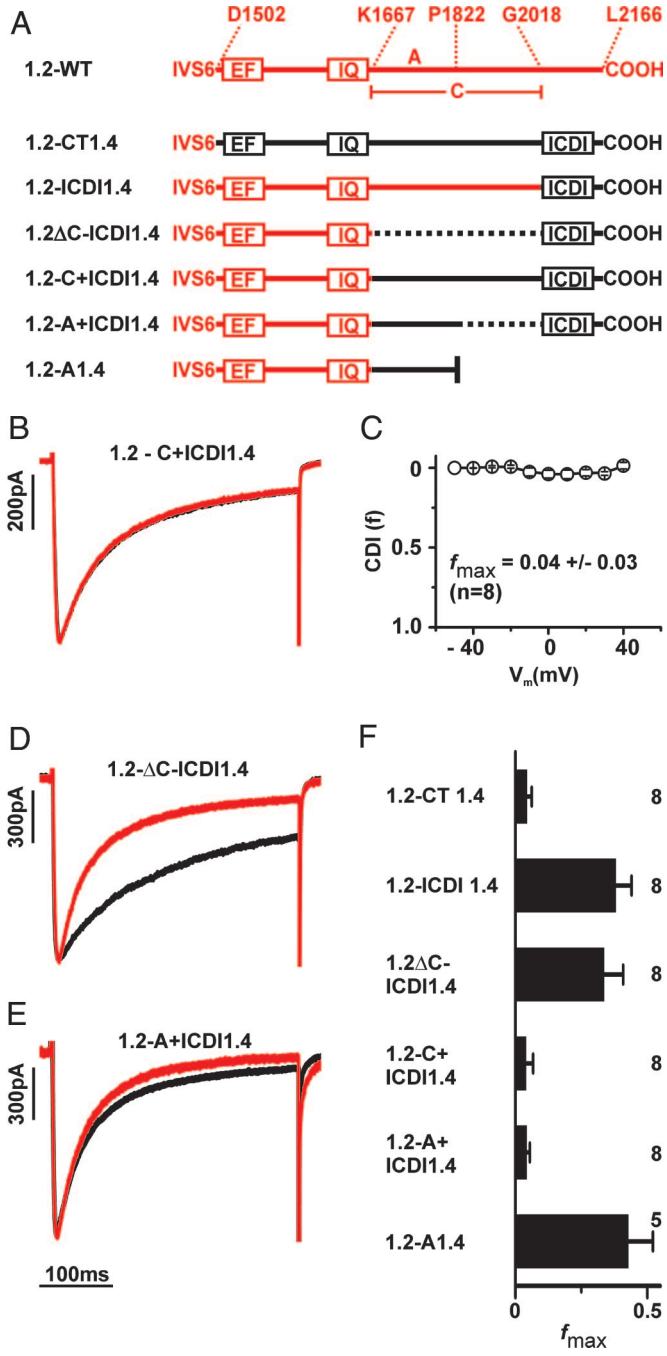

Fig. 4. The distal C terminus of Cav1.4 suppresses CDI in Cav1.2. (*A*) Schematic representation of Cav1.2-1.4 chimeric channels. Channel portions derived from Cav1.2 and Cav1.4 are displayed in red and black, representatively. Deletions are marked by dotted lines. (*B*) Representative I_{Ca} (red) and I_{Ba} (black) through 1.2-C+ICDI1.4. (*C*) Voltage-dependence of *f* for 1.2-C+ICDI1.4. (*D* and *E*) Representative I_{Ca} and I_{Ba} through 1.2ΔC-ICDI1.4 (*D*) and 1.2-A+ICDI1.4 (*E*). (*F*) f_{max} values for channels are shown in *A*.

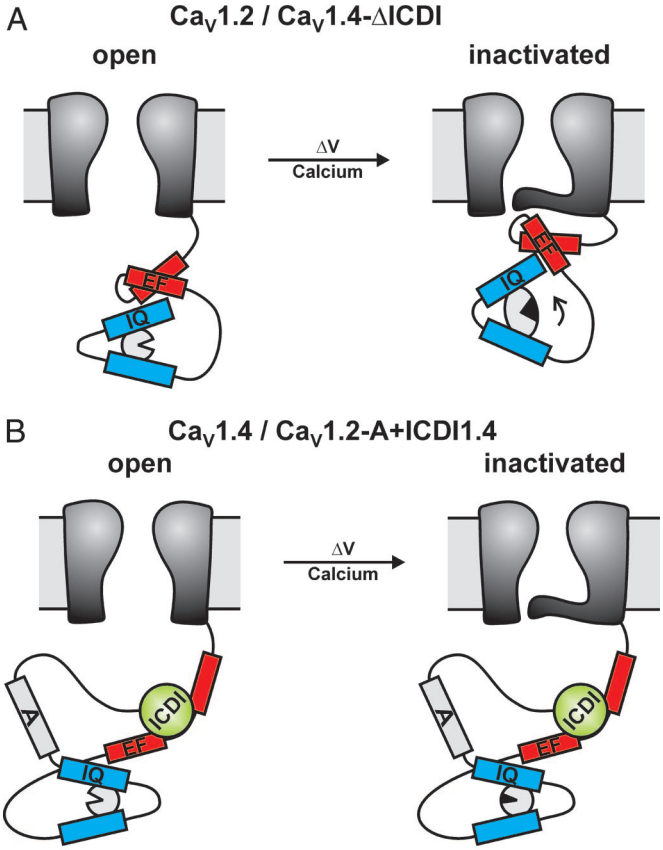

Fig. 5. Current (*A*) and extended (*B*) model of CDI. CaM and Ca^{2+} are displayed as a gray circle and black triangle, respectively. See *Discussion* for additional details.

hand (17, 29) that promotes an interaction between the EF hand motif and its target region(s) on the channel, thus conferring fast CDI (17, 29, 30). It is a matter of controversy where the interaction site of the EF hand is localized, but it may lie within the core (17, 29) or the linker between domains I and II of the channel (30–33). These channel domains are represented as a latch in Fig. 5. Our data extend this model to channels lacking CDI (Fig. 5*B*). We propose that in Cav1.4 and Cav1.2 carrying the distal C terminus of Cav1.4, ICDI constitutively binds to the EF hand motif. Hence, the conformational change in the EF hand is impaired, and inactivation occurs in a strictly voltage-dependent fashion with kinetics that are intrinsic to the respective channel core (very slow in Cav1.4 and fast in Cav1.2). Because the EF hand motif is uncoupled from the Ca^{2+}-sensing apparatus, the C terminus no longer can interact with its target regions. As a result, there is no CDI and inactivation is purely determined by voltage. This model is supported by the properties of a Cav1.2 deletion mutant lacking the EF hand motif (mutant 77dEF) (19). This channel completely lacks CDI and has inactivation time constants that are virtually identical to those of Cav1.2 carrying the distal C terminus of Cav1.4. The molecular details underlying the action of the A peptide of Cav1.4 are not yet known. This peptide is not sufficient but is required to block CDI in Cav1.2, suggesting that it supports the primary action of ICDI via an independent pathway. It is noteworthy to mention that unlike in Cav1.1 (34) and Cav1.2 (35), peptide A is not binding to the distal C terminus in Cav1.4. Quantitatively, the impact of peptide A is likely to be of minor importance because in Cav1.4, the peptide is not essential for blocking CDI.

Our findings also may have pathophysiological relevance. Loss-of-function mutations in the human Cav1.4 channel cause incomplete congenital stationary night blindness type 2 (CSNB2), an X-linked recessive disorder with symptoms of low visual acuity, myopia, nystagmus, and night blindness (10, 11, 36). In addition, two mutations in CSNB2 patients have been discovered, leading to channels with truncations in the distal C terminus that closely match truncations of murine Cav1.4 analyzed in the present study

(K1591X and R1816X corresponding to murine K1605X and R1834X, respectively; Fig. 6) (11, 37). Moreover, a frameshift mutation (5665delC; ref. 36) has been identified, resulting in the deletion of the sequence downstream of the first 10 aa of ICDI (Fig. 6). All three mutations leave the channel core and the Ca^{2+}-sensing apparatus intact but selectively remove ICDI. Our data strongly suggest that these human Cav1.4 mutants, if produced *in vivo*, very likely will display CDI and, hence, will cause a profound impairment of synaptic transmission in retinal cells, which explains the clinical phenotype.

Methods

Constructs for Electrophysiology. The rabbit Cav1.2b subunit (38) (GenBank accession no. X55763), chimeric channels based on Cav1.2 backbone, and a Ca^{2+}-insensitive CaM mutant harboring aspartate-to-alanine mutations in all four EF hands (CaM_{1234}) (26) were cloned into the pcDNA3 expression vector (Invitrogen, Carlsbad, CA). For expression of murine Cav1.4 (14) (accession no. AJ579852) and channels containing the Cav1.4 backbone, the bicistronic pIRES2-EGFP expression vector (Clontech, Mountain View, CA) was used. For the construction of truncated Cav1.4 channels (R1610Stop, Y1668Stop, R1796Stop, C1884Stop, Q1930Stop, and Q1953Stop), a fragment of the wild-type Cav1.4 expression plasmid was replaced by DNA fragments that are carrying the required stop codon and a restriction site introduced by 3′ primers. The ΔC channel was cloned by deleting amino acids R1610–C1884 of Cav1.4 by using overlap PCR. The following chimeric Cav1.2-1.4 channels also were generated by using overlap PCR (see also Fig. 4*A*): In 1.2CT1.4, D1502–L2166 of Cav1.2 was replaced by D1445–L1984 of Cav1.4; in 1.2-ICDI1.4, G2018–L2166 of Cav1.2 was replaced by L1885–L1984 of Cav1.4; in 1.2ΔC-ICDI1.4, K1667–L2166 of Cav1.2 was replaced by L1885–L1984 of Cav1.4; in 1.2-C+ICDI1.4, K1667–L2166 was replaced by R1610–L1984 of Cav1.4; in 1.2-A+ICDI1.4, K1667–L2166 of Cav1.2 was replaced by R1610–L1984 with a deletion of I1742–C1884 of Cav1.4. In 1.2-A1.4, K1667–L2166 of Cav1.2 was replaced by R1610–S1741 and a stop codon was introduced after S1741. See also Fig. 6 for alignment of the C termini of Cav1.2 and Cav1.4.

Electrophysiology. HEK293 cells were transiently transfected with expression vectors encoding calcium channel α subunits together with equimolar amounts of vectors encoding β2a and α2δ1 as described in ref. 14. I_{Ca} and I_{Ba} were measured by using the following solutions: (pipette solution) 112 mM CsCl/3 mM $MgCl_2$/3 mM MgATP/10 mM EGTA/5 mM Hepes, adjusted to pH 7.4 with CsOH; (bath solution) 82 mM NaCl/30 mM $BaCl_2$/5.4 mM $CsCl_2$/1 mM $MgCl_2$/20 mM tetraethylammonium/5 mM Hepes/10 mM glucose, adjusted to pH 7.4 with NaOH. For experiments with 10 mM Ba^{2+} or 10 mM Ca^{2+} in the bath solution the NaCl concentration was increased to 102 mM. I_{Ca} and I_{Ba} was measured from the same cell. Bath solution was changed by a local solution exchanger. Currents were recorded at room temperature 2–4 days after transfection by using whole-cell patch-clamp technique. Data were analyzed by using Origin 6.1 software (OriginLab, Northampton, MA).

The peak *I–V* relationship was determined by applying 350-ms voltage pulses to potentials between −80 and + 70 mV in 10-mV increments from a holding potential of −80 mV. The time course of current inactivation was fitted by the biexponential function: $I(t) = A_{fast} \times \exp(-t/\tau_{fast}) + A_{slow} \times \exp(-t/\tau_{slow}) + C$. τ_{slow} and τ_{fast} represent slow and fast time constants of inactivation, respectively. A_{slow} and A_{fast} are the amplitudes of the current components. A_{fast} (%) has been calculated as $A_{fast}/(A_{fast} + A_{slow}) \times 100$. I_{Ba} of Cav1.2, 1.2-ICDI1.4, and 1.2ΔC-ICDI1.4 was fitted best by the monoexponential function: $I(t) = A_0 \times \exp(-t/\tau) + C$, where $I(t)$ is the current at time t after a voltage pulse to V_{max}, A_0 the steady-state current amplitude with the respective time constant of inactivation, τ, and C, the remaining steady-state current. For I_{Ba} and I_{Ca} of Cav1.4α1, C1884Stop + CaM_{1234} and C1884Stop +ICDI and I_{Ba} of C1884Stop time course of inactivation was linear and, therefore, not fitted.

CDI was quantified by determining the f value essentially as described in ref. 39. Briefly, the fraction of peak Ba^{2+} and Ca^{2+} currents remaining after 300 ms of depolarization (r_{300}) was calculated. f is defined as the difference (r_{300} of I_{Ba}) − (r_{300} of I_{Ca}) and, hence, quantifies pure CDI. f can vary between 0 (no CDI) and 1 (complete CDI.) f was determined for various test potentials, and maximal f was taken for comparison of different channels.

Statistics. All values are given as mean ± SEM. n is the number of experiments. An unpaired t test was performed for the comparison between two groups. Significance was tested by ANOVA followed by Dunett test if multiple comparisons were made. Values of $P < 0.05$ were considered significant.

GST Pulldown of CaM. Sequences corresponding to C-terminal fragments of Cav1.2 [CT1.2-1667Stop (D1502–G1666); CT1.2-1667–2166 (K1667–L2166)] or Cav1.4 [CT1610Stop (D1445–G1609); CT1610–1984 (R1610–L1984)] were amplified by PCR and cloned into the pET41a bacterial expression vector (Novagen, Darmstadt, Germany) in frame with a N-terminal GST sequence. GST pulldowns were performed as described in ref. 17 with modifications specified in *Supporting Materials and Methods*, which is published as supporting information on the PNAS web site. Each GST pulldown was repeated at least three times.

ICDI Interaction Assay. Sequences corresponding to C-terminal fragments of Cav1.4 [CT1493Stop (D1445–I1492); CT1535Stop (D1445–V1534); CT1610Stop (D1445–G1609); and CT1610Stop,ΔEF (D1445–G1609, Δ P1459–I1492)] were amplified by PCR and cloned into the pET41a bacterial expression vector (Novagen) in frame with a N-terminal GST sequence. Flag-tagged ICDI-peptide (L1885-L1984) was cloned into pQE30 bacterial expression vector (Qiagen, Valencia, CA) by using primers containing the N-terminal flag sequence and the required restriction sites. GST pulldowns were performed as specified in *Supporting Text*. Each GST pulldown was repeated at least three times.

Co-IP in HEK293 Cells. The complete C terminus of Cav1.2 [CT1.2 (D1502–L2166)] or Cav1.4 [CT1.4 (D1445–L1984)] or C-terminal fragments of Cav1.4 [CT1610Stop (D1445–G1609); CT1610Stop,ΔEF (D1445–G1609, Δ P1459–I1492); peptide C (R1610–C1884); peptide A (R1610–S1741)] were amplified by PCR and cloned into the pcDNA3 expression vector. All sequences were fused with a myc tag at the N terminus. The triple flag-tagged ICDI peptide (L1885–L1984) and CaM_{1234} was constructed in the same manner by using a 5′ primer containing the triple flag sequence. For expression of recombinant proteins, HEK293 cells were transfected by using the calcium phosphate method. Immunoprecipitation was performed 3 days after transfection. A detailed protocol is available in *Supporting Materials and Methods*. Each Co-IP was repeated at least three times.

This work was supported by the Deutsche Forschungsgemeinschaft.

1. Wheeler DB, Randall A, Tsien RW (1994) *Science* 264:107–111.
2. Liang H, DeMaria CD, Erickson MG, Mori MX, Alseikhan BA, Yue DT (2003) *Neuron* 39:951–960.
3. Knapp AG, Dowling JE (1987) *Nature* 325:437–439.
4. Parsons TD, Sterling P (2003) *Neuron* 37:379–382.
5. Tachibana M, Okada T, Arimura T, Kobayashi K (1993) *Ann NY Acad Sci* 707:359–361.
6. Schmitz Y, Witkovsky P (1997) *Neuroscience* 78:1209–1216.
7. Yagi T, Macleish PR (1994) *J Neurophysiol* 71:656–665.
8. Protti DA, Llano I (1998) *J Neurosci* 18:3715–3724.

9. Berntson A, Taylor WR, Morgans CW (2003) *J Neurosci Res* 71:146–151.
10. Bech-Hansen NT, Naylor MJ, Maybaum TA, Pearce WG, Koop B, Fishman GA, Mets M, Musarella MA, Boycott KM (1998) *Nat Genet* 19:264–267.
11. Strom TM, Nyakatura G, Apfelstedt-Sylla E, Hellebrand H, Lorenz B, Weber BH, Wutz K, Gutwillinger N, Ruther K, Drescher B, *et al.* (1998) *Nat Genet* 19:260–263.
12. Heidelberger R, Thoreson WB, Witkovsky P (2005) *Prog Retin Eye Res* 24:682–720.
13. Morgans CW, Bayley PR, Oesch NW, Ren G, Akileswaran L, Taylor WR (2005) *Vis Neurosci* 22:561–568.
14. Baumann L, Gerstner A, Zong X, Biel M, Wahl-Schott C (2004) *Invest Ophthalmol Vis Sci* 45:708–713.
15. Koschak A, Reimer D, Walter D, Hoda JC, Heinzle T, Grabner M, Striessnig J (2003) *J Neurosci* 23:6041–6049.
16. McRory JE, Hamid J, Doering CJ, Garcia E, Parker R, Hamming K, Chen L, Hildebrand M, Beedle AM, Feldcamp L, *et al.* (2004) *J Neurosci* 24:1707–1718.
17. Peterson BZ, DeMaria CD, Adelman JP, Yue DT (1999) *Neuron* 22:549–558.
18. Zhou J, Olcese R, Qin N, Noceti F, Birnbaumer L, Stefani E (1997) *Proc Natl Acad Sci USA* 94:2301–2305.
19. Zuhlke RD, Reuter H (1998) *Proc Natl Acad Sci USA* 95:3287–3294.
20. Qin N, Olcese R, Bransby M, Lin T, Birnbaumer L (1999) *Proc Natl Acad Sci USA* 96:2435–2438.
21. Zuhlke RD, Pitt GS, Deisseroth K, Tsien RW, Reuter H (1999) *Nature* 399:159–162.
22. Pate P, Mochca-Morales J, Wu Y, Zhang JZ, Rodney GG, Serysheva II, Williams BY, Anderson ME, Hamilton SL (2000) *J Biol Chem* 275:39786–39792.
23. Romanin C, Gamsjaeger R, Kahr H, Schaufler D, Carlson O, Abernethy DR, Soldatov NM (2000) *FEBS Lett* 487:301–306.
24. Pitt GS, Zuhlke RD, Hudmon A, Schulman H, Reuter H, Tsien RW (2001) *J Biol Chem* 276:30794–30802.
25. Erickson MG, Liang H, Mori MX, Yue DT (2003) *Neuron* 39:97–107.
26. Xia XM, Fakler B, Rivard A, Wayman G, Johnson-Pais T, Keen JE, Ishii T, Hirschberg B, Bond CT, Lutsenko S, Maylie J, Adelman JP (1998) *Nature* 395:503–507.
27. Rost B, Sander C (1993) *J Mol Biol* 232:584–599.
28. Bernatchez G, Talwar D, Parent L (1998) *Biophys J* 75:1727–1739.
29. Peterson BZ, Lee JS, Mulle JG, Wang Y, de Leon M, Yue DT (2000) *Biophys J* 78:1906–1920.
30. Kim J, Ghosh S, Nunziato DA, Pitt GS (2004) *Neuron* 41:745–754.
31. Cens T, Restituito S, Galas S, Charnet P (1999) *J Biol Chem* 274:5483–5490.
32. Stotz SC, Hamid J, Spaetgens RL, Jarvis SE, Zamponi GW (2000) *J Biol Chem* 275:24575–24582.
33. Bernatchez G, Berrou L, Benakezouh Z, Ducay J, Parent L (2001) *Biochim Biophys Acta* 1514:217–229.
34. Hulme JT, Konoki K, Lin TW, Gritsenko MA, Camp DG, II, Bigelow DJ, Catterall WA (2005) *Proc Natl Acad Sci USA* 102:5274–5279.
35. Gao T, Cuadra AE, Ma H, Bunemann M, Gerhardstein BL, Cheng T, Eick RT, Hosey MM (2001) *J Biol Chem* 276:21089–21097.
36. Boycott KM, Maybaum TA, Naylor MJ, Weleber RG, Robitaille J, Miyake Y, Bergen AA, Pierpont ME, Pearce WG, Bech-Hansen NT (2001) *Hum Genet* 108:91–97.
37. Wutz K, Sauer C, Zrenner E, Lorenz B, Alitalo T, Broghammer M, Hergersberg M, de la Chapelle A, Weber BH, Wissinger B, *et al.* (2002) *Eur J Hum Genet* 10:449–456.
38. Biel M, Ruth P, Bosse E, Hullin R, Stuhmer W, Flockerzi V, Hofmann F (1990) *FEBS Lett* 269:409–412.
39. Mori MX, Erickson MG, Yue DT (2004) *Science* 304:432–435.